Studies of Chemisorbed Tetracene on Si(111)-7×7†

Kian Soon Yong,‡,§,# Yong Ping Zhang,‡ Shuo-Wang Yang,# Ping Wu,# and Guo Qin Xu*,‡

Department of Chemistry, National University of Singapore, 3 Science Drive 3, Singapore 117543, NUS Nanoscience and Nanotechnology Initiative, 2 Science Drive 3, Singapore 117542, and Institute of High Performance Computing, Singapore Science Park II, Singapore 117528

Received: June 14, 2007; In Final Form: August 13, 2007

The chemisorption of tetracene on the Si(111)-7×7 surface was studied using scanning tunneling microscopy (STM) and density functional theory (DFT) calculations. On the basis of the STM results and dimension analysis, two types of binding configurations were proposed. One of the configurations involves the di-σ reaction between two C atoms of an inner ring with an adatom−rest atom pair on the substrate to give rise to an unsymmetrical butterfly structure. Tetracene in another configuration possesses four C−Si bonds that are formed via di-σ reactions between the C atoms at the terminal rings with two center adatom−rest atom pairs within one-half of the surface unit cell. Besides, two other binding modes were proposed based on the dimension compatibility between the tetracene C and the substrate Si dangling bonds even though their identifications through the STM images are nonexclusive. Structural modeling and adsorption energies calculations were carried out using the DFT method. Factors affecting the relative thermodynamic stabilities based on the calculation results and the relative populations of tetracene in the different binding configurations as observed experimentally were discussed.

I. Introduction

The coupling of organic functionalities with the silicon surfaces creates new technological opportunities for fabrication of silicon-based organic−inorganic hybrid devices.[1−3] Such devices exploit the functional flexibility of organic molecules and the well-established silicon process technology to offer new and enhanced properties integrated to the silicon substrate. Among the organic molecules, linear acenes, particularly tetracene and pentacene, have been extensively studied and successfully employed for device fabrication.[4−7] Though tetracene, which has a planar structure that is comprised of four linearly fused benzene rings (Figure 1a), possesses a lower field-effect mobility than pentacene, it exhibits potential for use as light-emitting devices[4,7,8] and photodetectors.[6] Studies have been done to improve the film order of tetracene grown on various substrates[5,9−11] since both the charge transport and optical properties are influenced by the interactions between neighboring molecules and hence the morphology of the deposited film.[11,12] And in order to design the optimum conditions for growing tetracene on silicon, a thorough knowledge of the interfacial chemistry between tetracene and the silicon surface is critical because the first molecular layer on the substrate is going to affect the growth of subsequent tetracene molecules.

Rada and co-workers had studied the adsorption of tetracene on Si(100)-2×1 using scanning tunneling microscopy (STM).[13] Two bright and three dark distinctive features were observed in the filled and empty states STM images, respectively, whose orientations indicate that the tetracene adsorbates adopt flat-lying configurations on the surface and are aligned either parallel or perpendicular to the Si dimer rows. Furthermore, the authors proposed binding configurations for tetracene that involve two or four C−Si covalent bonds formed between the central C atoms on tetracene and the Si(100)-2×1 dimer row dangling bonds. In order to formulate such configurations, the reacted C atoms on tetracene change their hybridizations from sp^2 to sp^3, which results in the loss of aromaticities in the adsorbed molecules and the buckling of their planar ring structures.

On the other hand, the adsorptions of tetracene on Si(111)-7×7 and oxidized Si(111) surfaces had been studied by Schedel

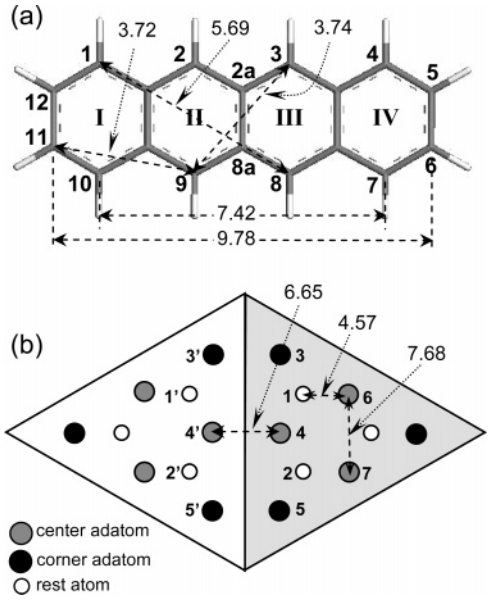

Figure 1. Dimensions, in units of angstrom, between various (a) carbon atoms on a tetracene molecule and (b) dangling bonds within a single unit cell (whose two different halves are distinguished by the shaded and unshaded triangles) of Si(111)-7×7. Some of the adatoms and rest atoms are labeled, and their locations on the different halves of the unit cell are differentiated by the primed and unprimed labels.

† Part of the "Giacinto Scoles Festschrift".

* Corresponding author. Fax: (65) 6779 1691. E-mail: chmxugq@nus.edu.sg.

‡ National University of Singapore.

§ NUS Nanoscience and Nanotechnology Initiative.

Institute of High Performance Computing.

10.1021/jp074627g CCC: $37.00
Published on Web 11/13/2007

et al. using near-edge X-ray absorption spectroscopy (NEXAFS).[14] Their result shows that tetracene adopts a flat-lying configuration on the Si(111)-7×7 surface. Similar to the Si(100)-2×1 surface, Si(111)-7×7 possesses reactive unsaturated dangling bonds that are expected to interact with the molecular π-orbitals on tetracene to form C−Si covalent bonds. Indeed, in the absence of the Si dangling bonds on the oxidized Si(111) surface, the NEXAFS result indicates that tetracene molecules adsorb at low coverages (1−2 monolayers) with the molecular planes almost perpendicular to the surface. Such adsorption configuration is a result of the reduced influence of the silicon surface on the adsorbates and the enhanced interactions between neighboring tetracene molecules.

However, unlike the Si(100)-2×1 surface where the Si dimer row dangling bonds are regularly arranged in straight rows and columns,[15] the dangling bonds on Si(111)-7×7 reside on the adatoms, rest atoms, and corner holes (Figure 1b) that are arranged in a more complex manner according to the dimer−adatom-stacking fault (DAS) model.[16] Hence, the interaction of tetracene with this surface is likewise expected to be more complicated as compared to the Si(100) surface. In order to achieve an atomistic understanding of the binding configurations of tetracene on Si(111)-7×7, investigation using techniques that offer atomic-scale information is imperative, which provides the impetus for the current study using STM combined with density functional theory (DFT) calculation.

In this paper, the results obtained from STM and DFT studies on the adsorption of tetracene on Si(111)-7×7 at room temperature are reported. The STM images reveal mainly adatom vacancies that are associated with the adsorption of tetracene. Through examination of these experimental results and analysis of the dimensions of the tetracene adsorbate and the surface Si atoms, two binding configurations of tetracene on Si(111)-7×7 are proposed. DFT studies were employed for structural modeling as well as calculations of the adsorption energies for these different binding modes. The major configuration is comprised of an unsymmetrical butterfly structure formed via di-σ reaction between two C atoms of an inner ring on tetracene with an adatom−rest atom pair on the substrate. This buckled structure allows electron π delocalization to take place on both sides of the reacted ring and thereby enhances the stability of the configuration. Tetracene in the thermodynamically more stable form possesses four C−Si bonds that are formed through di-σ reactions between the C atoms at the terminal rings with two center adatom−rest atom pairs within one-half of the surface unit cell. A coverage-dependent study on the proportions between the two configurations suggests that their relative populations are affected by a probability factor due to the number of available binding sites for adsorption. Additionally, two other binding modes were proposed based on the dimension compatibility between the tetracene C and the substrate Si dangling bonds. Identifications of these two configurations through STM images, however, are nonexclusive. A discussion on the chemistry behind the relative stabilities of the different binding configurations, based on theoretical calculations, is presented.

II. Experimental and Computational Details

The experiments were performed in an ultrahigh vacuum (UHV) chamber that is equipped with an Omicron variable temperature STM and has a base pressure better than 1×10^{-10} Torr. The sample used in the experiment was cut from a P-doped mirror-polished Si(111) wafer with a resistivity of 1−2 Ω·cm and a size of 12 mm × 2 mm × 0.5 mm. An atomically clean Si(111)-7×7 surface was prepared in situ using an annealing-only method. After an initial degassing at 650 °C for several hours, the sample was flashed to ∼1200 °C to remove the native surface oxide, followed by a quench to 950 °C and then slow cooling down to room temperature. This procedure routinely yields a clean and well-reconstructed Si(111)-7×7, as confirmed by STM. Tetracene (Sigma Aldrich) was dosed by sublimation from a tantalum crucible from which an attached thermocouple allowed the temperature to be monitored. Deposition of tetracene onto the clean silicon surface at room temperature was performed by resistive heating of the crucible to about 110 °C. Prior to dosing, the crucible and its contents were outgassed at about 115 °C. The STM images were acquired at room temperature in a constant-current mode with a tunneling current of 0.1 nA, and all voltages (V_s) reported in this paper were biased to the sample.

TABLE 1: Substrate Cluster Used for Computation, the Types of Surface Dangling Bonds That Are Involved in the Binding Interactions, and the DFT-Calculated Binding Energy for Each of the Tetracene Configuration on Si(111)-7×7

configurations	substrate clusters	surface dangling bonds attached to[a]	binding energies/eV
A1	$Si_{75}H_{50}$	UCe, URe	1.856
A2	$Si_{73}H_{50}$	UCo, URe	1.867
A3	$Si_{80}H_{52}$	FCe, FRe	1.856
A4	$Si_{75}H_{52}$	FCo, FRe	1.825
A1′	$Si_{71}H_{49}$	UCe, URe, FCo	1.259
A2′	$Si_{68}H_{47}$	UCo, URe, FCe	1.349
B1	$Si_{79}H_{52}$	2UCe, 2URe	2.449
B2	$Si_{81}H_{54}$	2FCe, 2FRe	2.260
C1	$Si_{80}H_{57}$	UCe, UCo, URe	1.953
C2	$Si_{83}H_{59}$	FCe, FCo, FRe	1.983
D1	$Si_{79}H_{58}$	UCe, FCe	1.535
D2	$Si_{76}H_{55}$	UCo, FCo	1.627

[a] U, unfaulted half; F, faulted half; Ce, center adatom; Co, corner adatom; Re, rest atom.

DFT calculations were carried out for structures modeling and adsorption energies calculations for the various binding configurations of tetracene on Si(111)-7×7. As a single Si(111)-7×7 unit cell comprising the base, dimer, rest atom, and adatom layers has 200 silicon atoms, it is computationally too costly to perform ab initio calculations on such a system. Therefore, clusters having a single tetracene molecule bonded to the corresponding adsorption sites were cut from a Si(111)-7×7 supercell built using the geometries as obtained from experimental result.[17] Cluster reduction was performed in such a way so as to enhance the characteristics of the reacting center and corner adatoms by having, respectively, their neighboring two and one rest atom retained in the cluster. The sizes of these clusters, which vary depending on the adsorption configurations, are listed in Table 1. Apart from the adatoms and rest atoms, these four Si layers clusters were terminated at the boundaries by hydrogen atoms.

The DFT calculations were performed using the DMol3 code[18] in Materials Studio (version 4.0.0.0) of Accelrys. The tetracene molecule, the reacting adatoms and rest atoms, and their immediate neighboring silicon atoms on the substrate were allowed to be optimized while the rest of the cluster atoms were frozen so as to simulate a bulklike environment. The adsorption energies for the different configurations were calculated by subtracting the energies of the clusters comprising the tetracene molecules and the substrates from the total energies of the free substrate clusters and gas-phase tetracene. In our calculations, the double-numeric quality basis set with polarization functions (DNP) and the generalized gradient approximation (GGA)

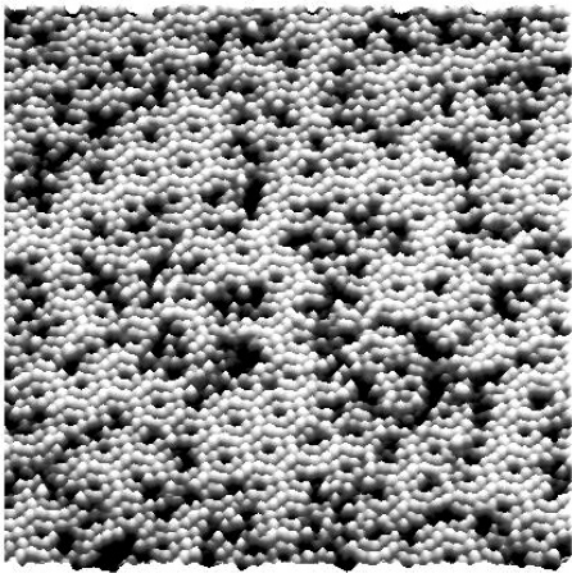

Figure 2. STM image (35×35 nm^2) of Si(111)-7×7 after submonolayer deposition of tetracene obtained at $V_s = 1.2$ V.

functional Perdew−Burke−Ernzerhof (PBE) developed by Perdew et al.[19] were employed. A real-space cutoff of 4.6 Å was applied, and a FINE quality mesh size of the program was used for the computation. The same set of parameters was used to calculate the binding energy of benzene chemisorbed in a 1,4-cyclohexadiene-like binding state on an adatom−rest atom pair simulated by a $Si_{49}H_{39}$ cluster. The energy of 0.92 eV obtained is in good comparison with other theoretical[20,21] and experimental[22,23] results.

III. Results and Discussion

III.A. Adsorption Configurations. Figure 2 shows a 35×35 nm^2 STM image of Si(111)-7×7 with submonolayer coverage of tetracene obtained at 1.2 V. On the reconstructed surface, the main features observable are adatoms vacancies. As the amount of such vacancies is much greater than the adatom vacancy defects (~1%) found on a clean Si(111)-7×7 surface, these features are characteristics of chemisorbed tetracene on the surface. The disappearance of the adatoms is a result of their reduced local density of states (LDOS) after reactions, and the invisibilities of the adsorbates can be accounted by the lack of low-lying energy states of the chemisorbed tetracene that are close to the Fermi level and accessible for tunneling. Such observations are also apparent in the empty state STM images for chemisorbed benzene on Si(111)-7×7, where each adatom vacancy is indicative of a benzene adsorption site.[23−26]

It has been well-established that benzene binds to Si(111)-7×7 through di-σ bond formations between C-1 and C-4 on benzene with an adatom−rest atom pair on the surface.[20−26] The structure of tetracene that is comprised of a benzene ring as the basic component is suggestive of a binding configuration of itself on Si(111)-7×7 that is similar to that of benzene on the same surface. This is further supported by the similarity between the empty state STM images of the two molecules on Si(111)-7×7, where adsorptions create adatom vacancies on the surface. Moreover, strong evidence of the participation of a Si adatom−rest atom pair in binding tetracene is shown in Figure 3. Figure 3a displays the STM image ($V_s = 1.6$ V) of an area of Si(111)-7×7 that had been exposed to tetracene. Upon changing the bias to −2.5 V, a sudden change in the tunneling condition occurred and caused the rest atoms to become clearly

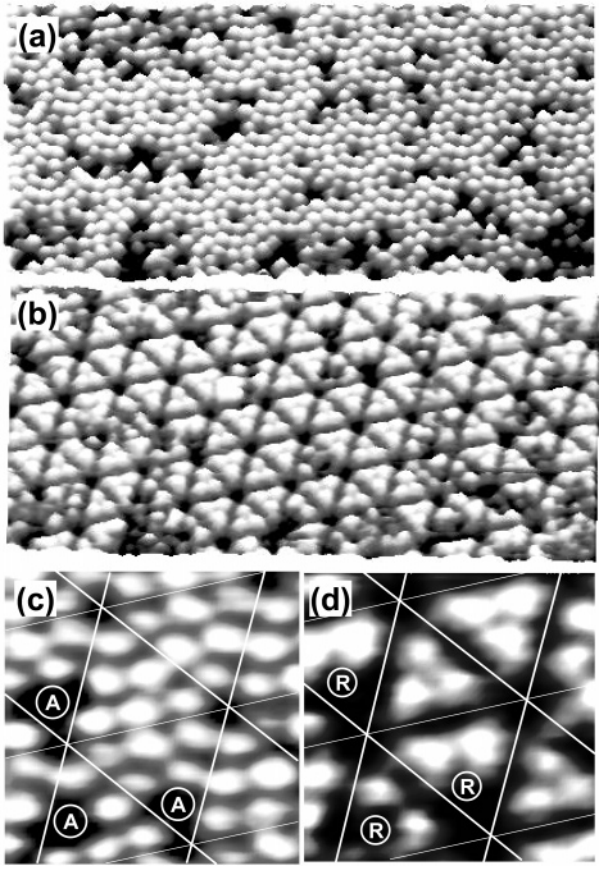

Figure 3. STM images of tetracene on Si(111)-7×7 at (a) 1.6 and (b) −2.5 V. The corresponding high-resolution images are shown in (c) and (d). Changing of the sample bias resulted in transformations of the surface features from adatoms in (a) to rest atoms in (b). The high-resolution images show simultaneous disappearance of adatoms (labeled "A" in (c)) and rest atoms (labeled "R" in (d)) that are adjacent to each other.

visible and the adatoms to almost disappear (Figure 3b). The reason for such an image brightness reversal is not clear, but this phenomenon had been observed before by Lo et al. in their study of H diffusion on Si(111)-7×7.[27] They proposed that changes in the tip surface due to transfer of atoms from the tip to the surface or vice versa could have resulted in the observations of these interesting images. Furthermore, they reasoned that the disappearance of some of the rest atoms was due to the adsorptions of H atoms.

The high-resolution images of Figure 3, parts a and b, are shown, respectively, in Figure 3, parts c and d. Individual triangular half-unit cells have been marked out by the white lines superimposed onto these images. In Figure 3c, the adatoms that disappeared are indicated by the circles that are labeled "A", whereas the missing rest atoms in Figure 3d are labeled "R". Interestingly, the "A" and "R" sites from the two images correspond to pairs of adatoms and rest atoms that are adjacent to each other. This result provides convincing evidence for the involvement of neighboring adatom−rest atom pair on Si(111)-7×7 in binding tetracene, which saturates the Si dangling bonds, alters their electronic density of states, and causes them to disappear from the STM images.

The appearance of tetracene in the STM images as adatom vacancies poses a challenge in the discernment of their adsorption characteristics on Si(111)-7×7. However, on the basis of NEXAFS results, Schedel et al. concluded the flat-lying configuration of molecular tetracene on Si(111)-7×7 at low coverages from the detection of the C 1s → π^* resonances.[14]

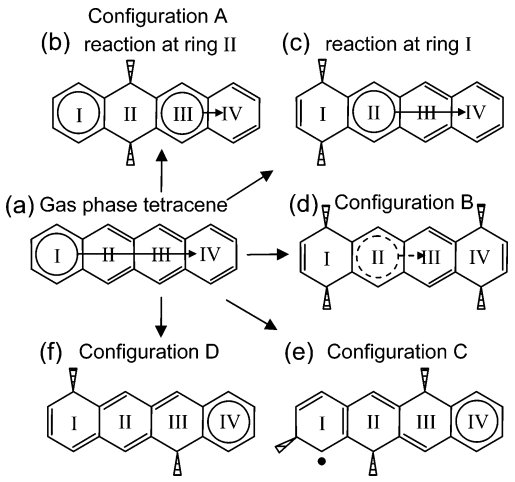

Figure 4. (a) Sharing of an aromatic sextet (represented by the circle in ring I) within tetracene via movement of two π electrons (symbolized by the arrow) according to Clar's sextet concept. Di-σ reactions at (b) ring II and (c) ring I of tetracene produce, respectively, two and one sextet in the resulting structure. (d) Loss of aromatic sextet due to nonplanar structure in configuration B of tetracene on Si(111)-7×7. (e) Tetracene in configuration C contains a radical site and possibly a sextet. (f) Reactions at rings I and III in configuration D result in isolation of a sextet to ring IV.

The molecular adsorption of tetracene may also be verified through comparison to studies of the adsorption of pentacene, the next higher acene member, on the same surface. The photoemission study from Hughes does not indicate any dissociation of pentacene on Si(111)-7×7.[28] Additionally, STM data show that chemisorbed pentacene appear as bright spots or dark depressed features that have dimensions comparable to that of molecular pentacene.[29]

Studies have shown that the [4 + 2] cycloaddition-like reaction involving C-1 and C-4 of benzene with an adjacent adatom−rest atom pair on Si(111)-7×7 is both thermodynamically and kinetically favorable over the [2 + 2] cycloaddition-like pathway that involves C-1 and C-2.[20,21] In a similar manner, the adatom−rest atom pair can interact with C-1 and C-10 of ring I or C-2 and C-9 of ring II on tetracene (C positions taken with reference from Figure 1a). However, experimental[30,31] and theoretical[32,33] studies have shown that the most reactive sites in tetracene for Diels−Alder reactions are the meso carbons of the inner rings (namely, C-2 and C-9 or the equivalent C-3 and C-8). These results may be explained qualitatively by Clar's sextet concept,[34,35] which represents tetracene as a π system that shares a single aromatic sextet having six π electrons. As illustrated in Figure 4a, this sextet is represented by the circle in ring I, which is mobile within the molecule via the movement of two π electrons as symbolized by the arrow. Apparently, reactions at the inner rings create species with two sextets located on both sides of the reacted ring (Figure 4b), whereas interactions at the outer rings result in only one sextet that is shared among the remaining three unreacted rings (Figure 4c). Hence the interaction of tetracene with the Si(111)-7×7 adatom−rest atom pair is expected to take place at the inner rings II or III to produce adsorbate that is hereafter referred to as type "A" configuration.

The DFT-optimized structures for the four types of configurations (referred to as configurations A1−A4) that are possible for type A binding mode are shown in Figure 5a−d. The notation for each cluster is detailed in the figure caption. The different species differ in the type of surface dangling bonds that they are attached to, as listed in Table 1. Additionally, Table 1 also provides the DFT-calculated binding energies for the various configurations. The calculated C−Si bond lengths for these clusters are in the range of 1.98−2.09 Å. The corresponding schematic diagram on the left of each cluster shows the attachment position of the tetracene molecule within a unit cell, where the shaded and unshaded triangles represent the faulted and unfaulted halves, respectively. Moreover, the center adatoms, corner adatoms, and rest atoms are denoted by the gray, black, and unfilled circles.

As shown in Figure 5a−d, the formations of covalent bonds between C-2 and C-9 of tetracene and the substrate adatom−rest atom pair, with the concomitant transformations of the reacting C atoms' hybridizations from sp^2 to sp^3, result in the unsymmetrical butterfly structures of configuration A. Such structures enhance the overlapping of the π-orbitals and in turn the aromaticity on both sides of the reacted ring. However, these structures differ from the one described by Rada and co-workers to explain the STM images of tetracene on Si(100)-2×1.[13] They proposed that the di-σ reaction with the substrate Si dimer takes place at the tetracene fusion C atoms at positions 2a and 8a (positions taken with reference from Figure 1a). In order to assess the stability of such a tetracene structure on Si(111)-7×7, DFT calculation was carried out for a cluster comprising a tetracene having C-2a and C-8a positioned close to a center adatom−rest atom pair on the unfaulted half. Optimization of the structure leads to a type A1 binding configuration for the tetracene adsorbate, indicating the instability of the structure that binds to the substrate with its fusion C atoms. This is in accordance with the result of a theoretical study to investigate the adsorption of acenaphthylene on Si(100)-2×1, which shows that di-σ reaction at the fusion C atoms within the naphthalene unit is thermodynamically unfavorable.[36] It is noted that the fusion carbons are attached to three other carbons from the tetracene backbone structure, whereas the nonfusion carbons have only two such neighboring carbon atoms and the valencies being fulfilled by hydrogen. The fusion carbons are therefore more rigid and expected to be more resistant toward transformation from the planar sp^2 to the tetragonal sp^3 hybridization.

Furthermore, the clusters for tetracene bonded to the unfaulted center or corner adatom−rest atom pair via di-σ reaction at C-1 and C-10 of ring I were also optimized and are presented in Figure 5, parts e and f, respectively. Apparently, the dimension of tetracene results in the proximity and hence the likely interaction between C-6 at the other terminal ring with a Si adatom on the other half of the unit cell. Such interaction would be expected to appear in the STM images via the simultaneous disappearance of a center (corner) adatom−rest atom pair and a corner (center) adatom on the other half of the unit cell. This combination of surface dangling bonds disappearance is, however, not observed in the set of STM results from Figure 3, for instance, and helps to support the validity of configurations A1−A4. The two different binding modes that occurred at the unfaulted center and corner adatoms were labeled as configurations A1′ and A2′, respectively, and their adsorption energies are shown in Table 1. Though three C−Si bonds were formed, tetracene in configurations A1′ and A2′ contains a radical site, which therefore reduces the stabilities of these structures as compared to configurations A1−A4.

As in the case of benzene adsorption on Si(111)-7×7,[24−26] the maximum number of tetracene with configuration A that can exist per half-unit cell is limited by the three rest atoms that are present. However, it is noted that no more than one tetracene in configuration A can bind simultaneously to two or three neighboring center adatoms, due to steric hindrance, as

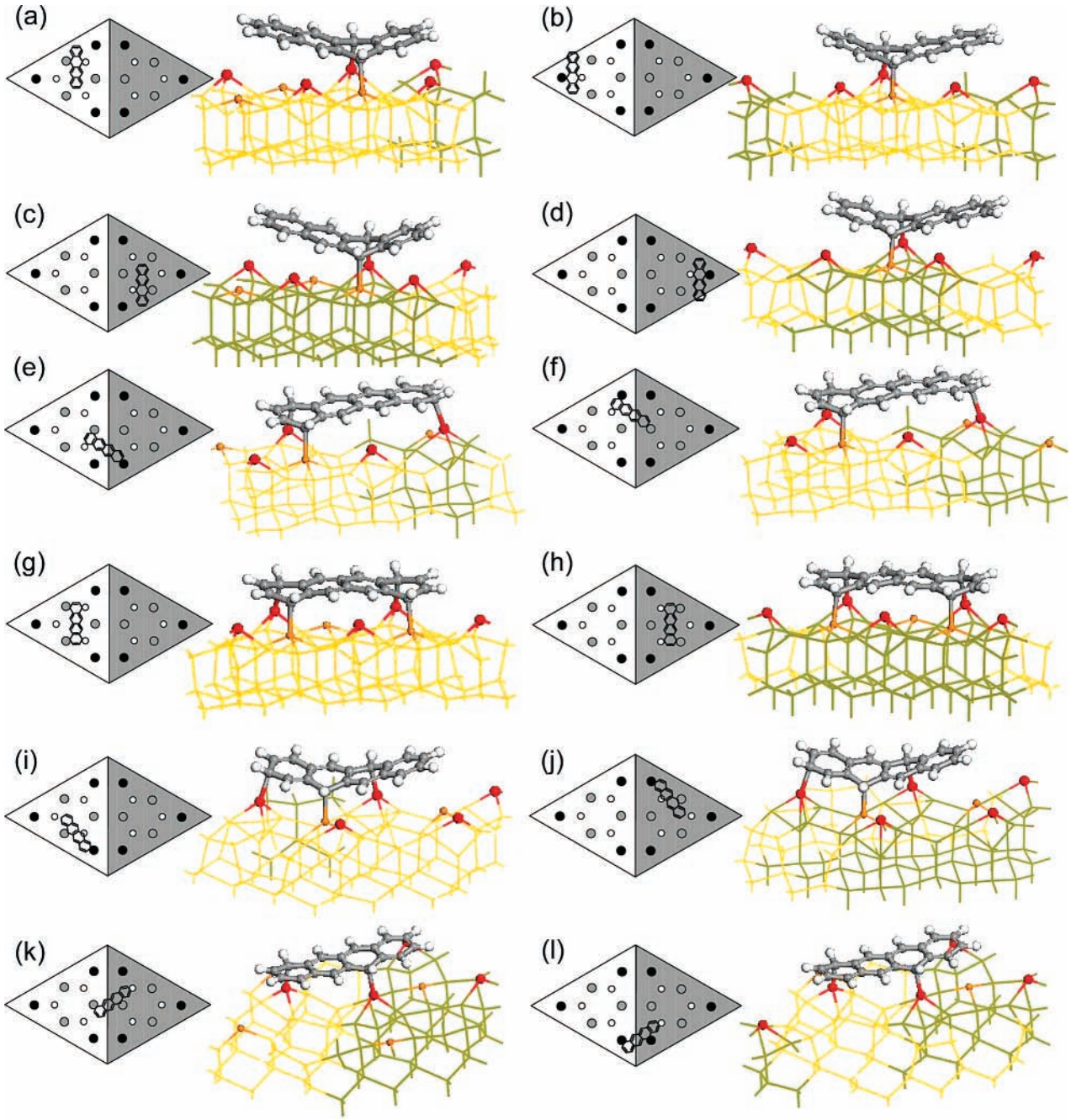

Figure 5. DFT-optimized structures for tetracene binding configurations (a) A1, (b) A2, (c) A3, (d) A4, (e) A1′, (f) A2′, (g) B1, (h) B2, (i) C1, (j) C2, (k) D1, and (l) D2 on Si(111)-7×7. Each cluster has the following notation: ball-and-stick, tetracene; yellow lines, unfaulted half; green lines, faulted half; red spheres, adatoms; orange spheres, rest atoms. The schematic diagram on the left of each cluster shows the attachment position of the tetracene molecule within a 7×7 unit cell, where the shaded and unshaded triangles represent the faulted and unfaulted halves, respectively.

exhibited in Figure 6. This figure shows the plan view of a tetracene molecule adsorbed with configuration A on a center adatom (Ce)−rest atom (Re) pair on the unfaulted half of Si(111)-7×7. This cluster, shown in black-and-white color scheme, has the same notation as that in Figure 5 except that the C atoms on tetracene that are bounded to the substrate adatom−rest atom pair have been distinguished by their darker shade in comparison with the unreacted C atoms. On the other two adjacent center adatoms, two imaginary tetracene molecules (represented by the broken and dotted lines) having butterfly structures have been inserted in two possible orientations with respect to the adsorbed tetracene as shown in the figure. The congestion at the central region shows that the dimension of the Si(111)-7×7 unit cell does not allow the occupations of tetracene adsorbates with type A configuration at two neighboring center adatoms at the same instant. Nevertheless, the disappearance of two center adatoms within a half-unit cell has been observed in the STM results, as shown in Figure 7b. It is proposed that such observation is due to tetracene in another binding mode, which is labeled as type "B" configuration.

From Figure 1a, the separation between C-1 and C-4 on tetracene is 7.42 Å, as obtained from our DFT calculations based on an isolated tetracene molecule. This distance is comparable to the separations of 7.68 Å between the two center adatoms as well as the two adjacent rest atoms[17] within a half-unit cell as shown in Figure 1b. Hence, it is proposed that tetracene in configuration B involves the interactions between C-1 and C-10 of ring I and C-4 and C-7 of ring IV with two neighboring

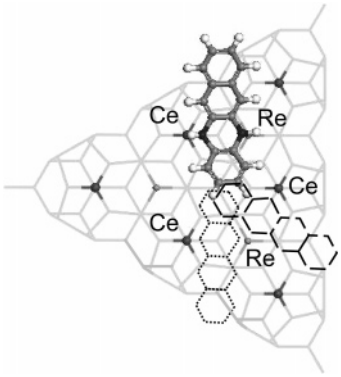

Figure 6. Cluster model (plan view) of a tetracene molecule bonded (with the two darkly shaded C atoms) to a center adatom (Ce)−rest atom (Re) pair with type A configuration on the unfaulted half of Si-(111)-7×7. Two imaginary tetracene molecules (represented in dotted and broken lines) were placed at the other adjacent center adatoms at two possible orientations with respect to the adsorbed tetracene. The congestion at the central region illustrates the impossibility for two neighboring center adatoms to bind two type A tetracene simultaneously.

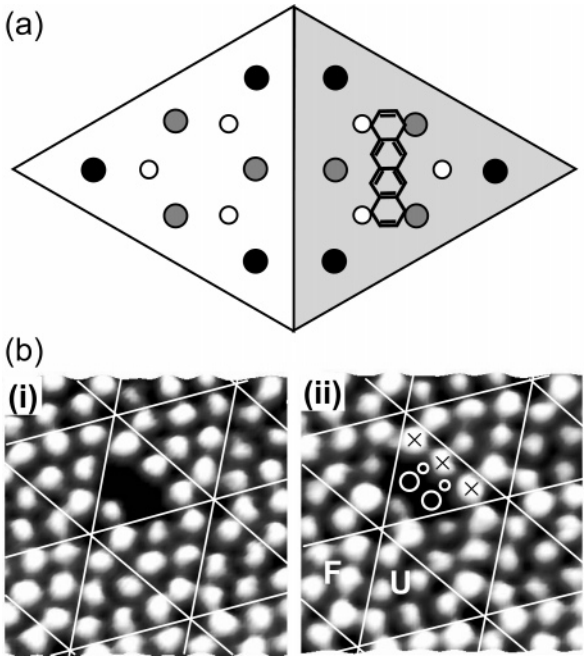

Figure 7. (a) Schematic diagram and (b) STM images of tetracene with type B binding configuration on Si(111)-7×7. In panel b, (i) and (ii) were obtained at $V_s = 1.5$ and -1.5 V, respectively, with F and U denoting the faulted and unfaulted half-unit cells.

pairs of center adatom−rest atom at surface dangling bonds 6, 1, 7, and 2, respectively. This binding configuration, as shown in the schematic diagram in Figure 7a, has four covalent bonds formed between tetracene and the surface. Moreover, two subconfigurations, labeled as B1 and B2 binding modes, are possible through reactions at the unfaulted and faulted halves of the 7×7 unit cell, respectively.

Parts i and ii of Figure 7b show, respectively, the STM images of tetracene in configuration B1 at $V_s = 1.5$ and -1.5 V. The white lines superimposed onto these images mark out the faulted (F) and unfaulted half (U) unit cells as distinguished by the filled state STM image in Figure 7b, part ii. The disappearance of the two center adatoms in Figure 7b, part i, indicates the adsorption of a tetracene in type B configuration, and the four circles in Figure 7b, part ii, denote the adatoms (larger circles) and rest atoms (smaller circles) that interacted with tetracene

TABLE 2: DFT-Calculated Values on the Differences ($\Delta Q = Q_{\text{tetracene/substrate}} - Q_{\text{substrate}}$) in the Mulliken Charges (In Electron Charge Units) on Some of the Substrate Atoms for Tetracene Binding Configuration B1 on Si(111)-7×7[a]

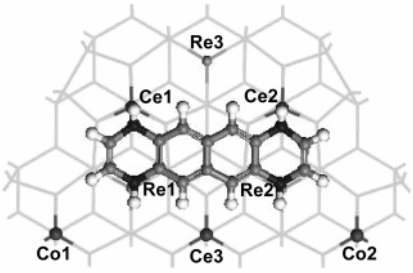

	Ce1	Ce2	Ce3	Co1	Co2	Re1	Re2	Re3
ΔQ	0.212	0.208	−0.141	−0.079	−0.064	0.253	0.258	−0.031

[a] Ce, center adatom; Co, corner adatom; Re, rest atom.

to form covalent bonds. Furthermore, it can be observed from Figure 7b, part ii, that the three neighboring adatoms (marked by the crosses) on an unfaulted half-unit cell have greater brightness as compared to the adatoms in the other unfaulted half-unit cells that have no reaction. This increase in charge density indicates a transfer of charges from their neighboring rest atoms (the two small circles) following their reactions with tetracene, thereby providing evidence for the participations of the rest atoms in binding tetracene in configuration B. Such movement of electrons through the back-bonds facilitates the reaction of the rest atoms, via removal of their excess charges,[37] with tetracene, which has also been observed in other reactions, such as that of NH_3 with Si(111)-7×7.[38] It is noted that pentacene, the next higher acene member, possesses a similar adsorption configuration on Si(111)-7×7, except for the isolation of an aromatic sextet to the outer ring that was not involved in the binding reaction.[29] However, unlike pentacene, which is visible as a depressed feature in the STM images, tetracene in configuration B cannot be distinguished at the same bias in the STM images. This difference could be attributed to the dissimilarity in the electronic structures of the two adsorbates, with pentacene having higher LDOS, relative to tetracene, that are close to the Fermi level. However, further studies for investigating the electronic structures of the two adsorbates on Si(111)-7×7 are necessary to gain insight to the difference between the two systems.

The DFT-optimized clusters for type B1 and B2 configurations are shown, respectively, in Figure 5, parts g and h, and their calculated binding energies are listed in Table 1. Apparently, tetracene in these configurations is almost parallel to the surface except for the slight tilt toward the rest atoms due to the approximate 1 Å height difference between the adatom and the rest atom.[17] Furthermore, a sextet that is shared between rings II and III can be identified in these configurations, as shown in Figure 4d. However, it is apparent from Figure 5, parts g and h, that rings II and III deviate slightly from planarity due to the conversions of the hybridizations of C-1 and C-10 of ring I and C-4 and C-7 of ring IV from sp^2 to sp^3. The resultant structure would impede the efficient overlapping of the π-orbitals within the sextet, thereby causing a loss in aromaticity.

Table 2 presents the calculated Mulliken charge differences (ΔQ) on some of the substrate atoms for the optimized configuration B1 cluster shown (in plan view) above the table. This cluster, shown in black-and-white color scheme, has the same notation as those in Figure 5 except that the tetracene C atoms that have covalent bonds with the substrate Si atoms are

darkly shaded. Ce, Co, and Re represent, respectively, the substrate center and corner adatoms and the rest atoms. Due to the perspective of the presentation, the four substrate atoms that bind tetracene, namely, Ce1, Ce2, Re1, and Re2, are being blocked from view by the adsorbed tetracene. ΔQ is obtained by subtracting the charges on the clean surface atoms from those on the corresponding atoms of the adsorbate/substrate cluster. Apparently, charges were transferred to the three unreacted adatoms (namely, Ce3, Co1, and Co2) from their neighboring reacted rest atoms (Re1 and Re2). This observation agrees with the negative bias STM images shown in Figure 7b, part ii, where the charge density increases in the three unreacted adatoms are evidenced by their intensified brightness in the images.

Being a large molecule relative to the distances between the dangling bonds on Si(111)-7×7, it is likely for tetracene to bind to the surface with other types of configurations which cannot be easily resolved based on the STM results. On the basis of the dimension compatibility between the tetracene C and the substrate Si dangling bonds, two other possible binding configurations were proposed. These configurations, labeled as type "C" and "D" configurations, are shown in Figure 5. Furthermore, the DFT-calculated adsorption energies for these binding modes are tabulated in Table 1.

Figure 5, parts i and j, displays two possible configurations (C1 and C2) for type C binding mode due to adsorptions at the unfaulted and faulted halves, respectively. Apparently, three C−Si covalent bonds can be formed between C-11, C-3, and C-9 on tetracene and the Si dangling bonds at positions 3, 6, and 1, respectively. The C and Si positions are taken with reference from Figure 1, which also exhibits the comparable distances of C11−C9 (3.72 Å) and C3−C9 (3.74 Å) with the center or corner adatom−rest atom separation (4.57 Å). Due to the odd number of C−Si bonds that are formed in this configuration, a radical site is present within the tetracene adsorbate. Furthermore, the formation of an aromatic sextet at the isolated ring IV that was not involved in the binding reaction is also possible, as shown in Figure 4e.

On the other hand, tetracene in type D configuration adsorbs on the surface via two C−Si covalent bonds that are formed between C-1 and C8 on tetracene with an unfaulted and a faulted adatom that are adjacent to each other. As depicted in Figure 5, parts k and l, reactions at the center−center adatoms (4′−4) and corner−corner adatoms (5′−5) give rise to configurations D1 and D2, respectively. The separations of 6.65 Å between these adatom pairs are comparable to the distance of 5.69 Å between C-1 and C-8 on tetracene. As shown in Figure 4f, such adsorption configuration also results in the formation of an aromatic sextet in ring IV, which would contribute to the stabilization of the structure.

Assuming that both configurations C and D, if present, also result in adatom vacancy-like feature in the STM image as in the case of configurations A and B, configuration C would appear as a pair of disappeared neighboring center−corner adatoms, whereas configuration D would appear as a pair of adjacent adatom vacancies with one on each half of the 7×7 unit cell. Though such surface features are observed in the STM images, they do not point exclusively to the presence of configurations C and D. Furthermore, it is apparent from Figure 5 that tetracene in binding modes A−D are almost parallel to the substrate, which agrees with the NEXAFS result from Schedel et al. regarding the flat-lying configurations of tetracene on the same surface at low coverages.[14]

III.B. Adsorption Energies and Relative Populations. Among type A and B binding configurations for tetracene on Si(111)-7×7, it can be observed from Table 1 that the latter has higher adsorption energy. This greater stability may be attributed to the four C−Si covalent bonds that are present in this configuration, as compared to type A binding mode that is comprised of only two such bonds. Furthermore, the B1 configuration that is located at the unfaulted half-unit cell is slightly more stable than B2 at the faulted half. On the basis of Brommer's concepts of local softness and electronegativity with regard to the relative reactivities of the dangling bonds on Si(111)-7×7,[39] electron-donating species would prefer to react with the center adatoms on the faulted as compared to the unfaulted half. Hence, the opposite behavior, that is reaction with the unfaulted center adatoms, is expected to be observed for electron-accepting species. In order to assess the charge transfer between the tetracene adsorbate and the Si surface, the Mulliken charge difference obtained by subtracting the charges on an isolated tetracene molecule from those in the adsorbate with configuration B1 on the Si surface was calculated. The total charge balance points to a charge transfer of ∼0.79 e from the substrate to the adsorbate, indicating that tetracene is an electron acceptor with respect to Si(111)-7×7. On the basis of the above reasoning and calculation result, tetracene in configuration B, having the center adatoms as the binding sites, would thus be expected to be more stable in configuration B1 by residing on the unfaulted half of the unit cell.

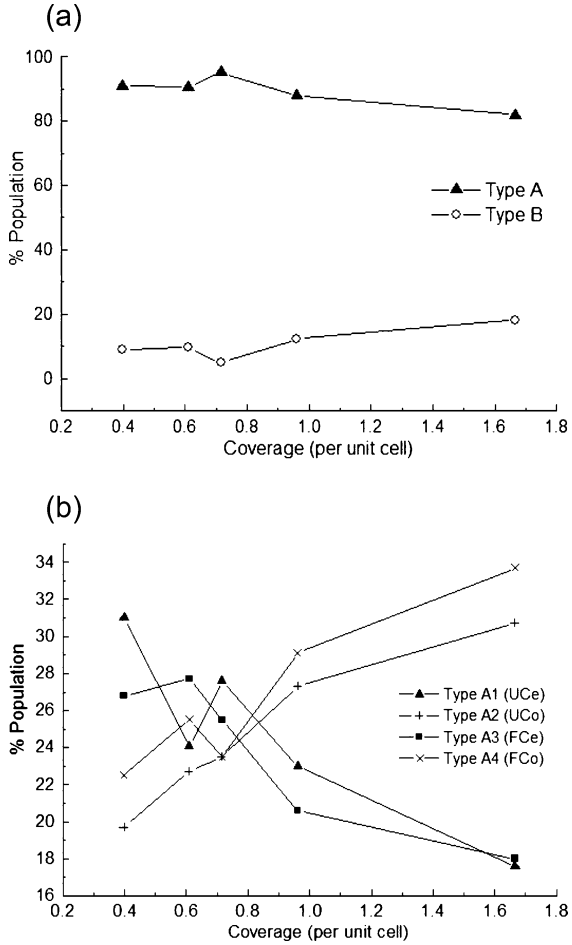

Figure 8. Proportions of tetracene in configurations (a) A and B and (b) A1, A2, A3, and A4 on Si(111)-7×7 at different surface coverages.

The proportions of tetracene in configurations A and B at different coverages as observed from our STM studies are presented in Figure 8a. The coverage was calculated by dividing the total number of tetracene in the different configurations by the number of 7×7 unit cells that were scanned. For example,

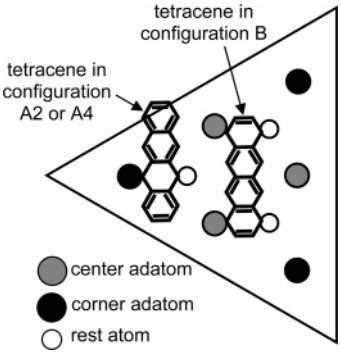

Figure 9. Binding of tetracene in configuration B on a 7×7 half-unit cell obstructs binding for A1 or A3 configuration at the center adatom−rest atom site but still allows an incoming tetracene to adsorb with A2 or A4 configuration on the remaining unreacted corner adatom−rest atom site.

at the highest coverage of 1.69 per unit cell as depicted in Figure 8a, the numbers of tetracene in type A and B configurations found within a total number of about 196 unit cells (∼35 × 35 nm^2) are 270 and 62, respectively. Apparently the dominant adsorption configuration for tetracene on Si(111)-7×7 is type A, whose amount shows a gradual decreasing trend with increasing coverage. In contrast, it is apparent that type B configuration exhibits a general increasing trend as the coverage increases.

Figure 8b shows the proportion of type A1−A4 configurations at different coverages calculated using the method as described above. Despite of some irregularities at the initial coverages, binding modes with tetracene occupying the center adatoms (type A1 and A3 configurations) are observed to be generally decreasing with increase in coverage, as contrast to the bindings that take place at the corner adatoms (A2 and A4 configurations), which exhibit the opposite behaviors. Furthermore, these decreasing (increasing) trends for type A1 and A3 (A2 and A4) configurations correspond directly with that for configuration A (configuration B) in Figure 8a. It is interesting to note that the presence of a tetracene in configuration B would result in the total loss of the center adatom−rest atom binding sites for tetracene in configuration A1 or A3 within a 7×7 half-unit cell. On the other hand, the remaining unreacted corner adatom−rest atom pair would still allow binding reaction to take place to form A2 or A4 configuration, as illustrated in Figure 9. Hence, an increase in the proportion of type B binding mode would have a larger influence on slowing down the growth in the amount of type A1 or A3 configuration as compared to that for type A2 or A4 as the tetracene coverage increases. In contrast, no obvious trend was observed for configurations B1 and B2. Additionally, it is noted that diffusion of the adsorbates and conversions between type A and B species were not observed between consecutive scans in the STM experiments. Therefore, the relative populations of tetracene in the different binding configurations that are present experimentally cannot be accounted for by thermodynamic factors.

Figure 10 illustrates the number of possible adsorption sites when a tetracene molecule initially interacts with a 7×7 unit cell to form the different binding configurations. The numbers of binding sites are 18 and 6 for type A and B configurations, as shown in Figure 10, parts a and b, respectively. Furthermore, it is noted that the binding of a tetracene in configuration B permits the adsorption of only one more tetracene with the same configuration within a unit cell. In contrast, it is possible for a unit cell to accommodate up to six tetracene molecules of type A configuration. Hence one of the possible reasons for the domination of type A species may be due to the much higher number of adsorption sites that are available for this species.

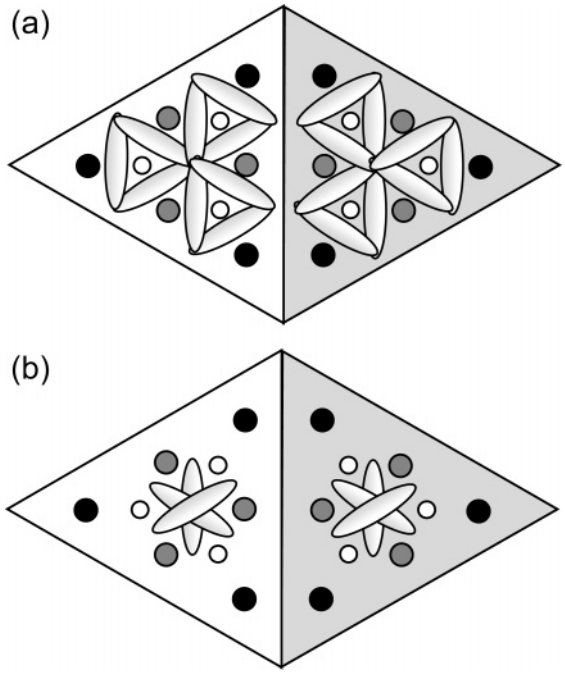

Figure 10. Si(111)-7×7 unit cells with each elongated oval within each unit cell representing a single tetracene molecule lying at a possible binding site for type (a) A and (b) B configurations. Hence, the numbers of initial adsorption sites available for a tetracene molecule to interact with a unit cell are 18 and 6 for type A and B binding modes, respectively.

From Table 1, tetracene in configuration C, if present, has the second highest adsorption energy after configuration B. Such relatively stable structure may be attributed to the presence of three C−Si covalent bonds as well as the aromatic sextet within the structure, despite the existence of a destabilizing radical in the tetracene adsorbate. On the other hand, type D species is thermodynamically less stable than type A species, even though they possess the same number of C−Si covalent bonds. One likely reason could be due to the presence of the two aromatic sextets that are found within configuration A, as compared to only one such stabilizing factor in configuration D. Additionally, the unsymmetrical adsorption configuration in type D binding mode could have induced strain and thereby destabilized the binding structure as compared to type A configuration.

IV. Conclusions

The chemisorbed species of tetracene on Si(111)-7×7 at room temperature were studied using STM and DFT calculations. On the basis of the STM images and the analysis of the dimension compatibility between the various Si dangling bonds and the tetracene C atoms, two types of tetracene binding modes were proposed. DFT studies were employed for structural modeling and adsorption energies calculations for the two different configurations. Tetracene in the major configuration involves the di-σ reaction between two C atoms of an inner ring with an adatom−rest atom pair on the substrate to give rise to an unsymmetrical butterfly structure. This buckled structure allows electron π delocalization to take place on both sides of the reacted ring and thereby enhances the stability of the configuration. The other binding mode for tetracene on Si(111)-7×7, which is thermodynamically more stable, is comprised of four C−Si covalent bonds that are formed through di-σ reactions between the C atoms at the terminal rings with two center adatom−rest atom pairs within one-half of the surface unit cell. A coverage-dependent study suggests that the relative popula-

tions of the two species are affected by a probability factor due to the number of available binding sites for adsorption. Besides the two configurations, another two possible binding modes for tetracene adsorption on Si(111)-7×7 were proposed. However, identifications of these binding modes through STM images are nonexclusive and their possible existence is based on the dimension compatibility between some of the C atoms on tetracene and the dangling bonds on Si(111)-7×7. In one of the configurations, the formation of bonds between three C atoms on tetracene and two adatoms and one rest atom on the substrate results in a radical site and also possibly an aromatic sextet within the tetracene adsorbate. The other configuration, on the other hand, is comprised of two C−Si covalent bonds and a sextet of six π electrons in an isolated ring that was not involved in the binding reaction. The relative stabilities of the different configurations as calculated may qualitatively be accounted for by collective effects due to factors such as the number of C−Si bonds formed, the preservation of aromaticity, and the extent of geometric strain induced within the bound molecule.

Acknowledgment. This project was supported by the Ministry of Education, Singapore (R-143-000-250-112).

References and Notes

(1) Yates, J. T., Jr. *Science* **1998**, *279*, 335.
(2) Wolkow, R. A. *Annu. Rev. Phys. Chem.* **1999**, *50*, 413.
(3) Bent, S. F. *Surf. Sci.* **2002**, *500*, 879.
(4) Hepp, A.; Heil, H.; Weise, W.; Ahles, M.; Schmechel, R.; Seggern, H. v. *Phys. Rev. Lett.* **2003**, *91*, 157406.
(5) Abthagir, P. S.; Ha, Y.-G.; You, E.-A.; Jeong, S.-H.; Seo, H.-S.; Choi, J.-H. *J. Phys. Chem. B* **2005**, *109*, 23918.
(6) Choi, J.-M.; Lee, J.; Hwang, D. K.; Kim, J. H.; Im, S. *Appl. Phys. Lett.* **2006**, *88*, 043508.
(7) Santato, C.; Manunza, I.; Bonfiglio, A.; Cicoira, F.; Cosseddu, P.; Zamboni, R.; Muccini, M. *Appl. Phys. Lett.* **2005**, *86*, 141106.
(8) Muccini, M. *Nat. Mater.* **2006**, *5*, 605.
(9) Campione, M.; Sassella, A. *J. Chem. Phys.* **2006**, *124*, 224705.
(10) Shi, J.; Qin, X. R. *Phys. Rev. B* **2006**, *73*, 121303(R).
(11) Soubatch, S.; Temirov, R.; Weinhold, M.; Tautz, F. S. *Surf. Sci.* **2006**, *600*, 4679.
(12) Cornil, J.; Beljonne, D.; Calbert, J.-P.; Brédas, J.-L. *Adv. Mater.* **2001**, *13*, 1053.
(13) Rada, T.; Chen, Q.; Richardson, N. V. *J. Phys.: Condens. Matter* **2003**, *15*, S2749; *Phys. Status Solidi B* **2004**, *241*, 2353.
(14) Schedel, Th.; Frank, K.-H.; Karisson, U.; Koch, E. E. *Vacuum* **1990**, *41*, 652.
(15) Tromp, R. M.; Hamers, R. J.; Demuth, J. E. *Phys. Rev. Lett.* **1985**, *55*, 1303.
(16) Takayanagi, K.; Tanishiro, Y.; Takahashi, M.; Takahashi, S. *J. Vac. Sci. Technol., A* **1985**, *3*, 1502.
(17) Tong, S. Y.; Huang, H.; Wei, C. M.; Packard, W. E.; Men, F. K.; Glander, G.; Webb, M. B. *J. Vac. Sci. Technol., A* **1988**, *6*, 615.
(18) Delley, B. *J. Chem. Phys.* **1990**, *92*, 508; *J. Chem. Phys.* **2000**, *113*, 7756; *Comput. Mater. Sci.* **2000**, *17*, 122.
(19) Perdew, J. P.; Burke, K.; Ernzerhof, M. *Phys. Rev. Lett.* **1996**, *77*, 3865.
(20) Wang, Z. H.; Cao, Y.; Xu, G. Q. *Chem. Phys. Lett.* **2001**, *338*, 7.
(21) Lu, X.; Wang, X.; Yuan, Q.; Zhang, Q. *J. Am. Chem. Soc.* **2003**, *125*, 7923.
(22) Cao, Y.; Wei, X. M.; Chin, W. S.; Lai, Y. H.; Deng, J. F.; Bernasek, S. L.; Xu, G. Q. *J. Phys. Chem. B* **1999**, *103*, 5698.
(23) Wolkow, R. A.; Moffatt, D. J. *J. Chem. Phys.* **1995**, *103*, 10696.
(24) Kawasaki, T.; Sakai, D.; Kishimoto, H.; Akbar, A. A.; Ogawa, T.; Oshima, C. *Surf. Interface Anal.* **2003**, *31*, 126.
(25) Tomimoto, H.; Takehara, T.; Fukawa, K.; Sumii, R.; Sekitani, T.; Tanaka, K. *Surf. Sci.* **2003**, *526*, 341.
(26) Tomimoto, H.; Sekitani, T.; Sumii, R.; Sako, E. O.; Wada, S.-i.; Tanaka, K. *Surf. Sci.* **2004**, *566*−*568*, 664.
(27) Lo, R.-L.; Ho, M.-S.; Hwang, I.-S.; Tsong, T. T. *Phys. Rev. B* **1998**, *58*, 9867.
(28) Hughes, G.; Carty, D.; Cafolla, A. A. *Surf. Sci.* **2005**, *582*, 90.
(29) Yong, K. S.; Zhang, Y. P.; Yang, S. W.; Wu, P.; Xu, G. Q. *J. Phys. Chem. C* **2007**, *111*, 4285.
(30) Biermann, D.; Schmidt, W. *J. Am. Chem. Soc.* **1980**, *102*, 3163.
(31) Murata, Y.; Kato, N.; Fujiwara, K.; Komatsu, K. *J. Org. Chem.* **1999**, *64*, 3483.
(32) Schleyer, P. v. R.; Manoharan, M.; Jiao, H.; Stahl, F. *Org. Lett.* **2001**, *3*, 3643.
(33) Cheng, M. F.; Li, W.-K. *Chem. Phys. Lett.* **2003**, *368*, 630.
(34) Clar, E. *Polycyclic Hydrocarbons*; Academic Press: London, 1964; Vol. 1 and 2.
(35) Clar, E. *The Aromatic Sextet*; Wiley: London, 1972.
(36) Nunzi, F.; Sgamellotti, A.; Re, N. *J. Phys. Chem. B* **2004**, *108*, 10881.
(37) Northrup, J. E. *Phys. Rev. Lett.* **1986**, *57*, 154.
(38) Avouris, Ph.; Wolkow, R. *Phys. Rev. B* **1989**, *39*, 5091.
(39) Brommer, K. D.; Galván, M.; Dal Pino, A., Jr.; Joannopoulos, J. D. *Surf. Sci.* **1994**, *314*, 57.